Copyright © 2005 by ABCM

COMPUTATIONAL ANALYSIS OF THE AIR FLOW AROUND A COMMERCIAL BUS MODEL

André Luiz Carregari
USP - Universidade de São Paulo
Escola de Engenharia de São Carlos - Depto. de Engenharia de Materiais, Aeronáutica e Automobilística
Av. Trabalhador Sancarlense, 400 - SP - 13566-590 - Brasil
carregari@gmail.com

Paulo Celso Greco Júnior
USP - Universidade de São Paulo
Escola de Engenharia de São Carlos - Depto. de Engenharia de Materiais, Aeronáutica e Automobilística
Av. Trabalhador Sancarlense, 400 - SP - 13566-590 - Brasil
pgreco@sc.usp.br

Abstract. *Two main reasons for improving aerodynamic characteristics of road vehicles are reducing fuel consumption and improving engine refrigeration. These objectives can be achieved with the adjustment of vehicle aerodynamic surfaces and with the use of aerodynamic devices. In the present study a numerical simulation commercial software is used to analyze the air flow around a 1/17.5 scale bus model. The Reynolds averaged Navier-Stokes equations are solved using the finite volume method with an RNG κ-ε turbulence model. Results show a complex wake structure behind the bus and also improvements in aerodynamic drag obtained with modifications in the bus external geometry.*

Keywords: *drag coefficient, RNG κ-ε turbulence model, commercial bus, turbulent wake.*

1. Introduction

The analysis of aerodynamic characteristics can be conducted using experimental methods. Such methods are usually money and time expensive for they may involve model construction, instrumentation, wind tunnel testing or road testing. The use of computational tools yields cost reduction and greater flexibility in the aerodynamic analysis of road vehicles. It is necessary, however, to verify computational results against the greatest possible number of test cases in an attempt to adequately choose and adjust the mathematical simulation model. Computational Fluid Dynamics (CFD) is becoming an essential tool in the development of new vehicles.

The air flow around a road vehicle is very complex but it is a well established fact that modifications in external geometry can yield significative reduction in aerodynamic drag. However, design constraints in internal volume and vehicle size restrict the extent of those modifications. One of the major difficulties in designing passenger or cargo commercial road vehicles is related to fuel consumption. A bus traveling at 80 km/h spends approximately 46% of fuel with aerodynamic drag and 54% with rolling resistance. Fuel consumption and engine refrigeration are two main concerns in the study of road vehicle aerodynamics which can be improved through modification of external vehicle geometry and through the use of aerodynamic devices.

Several studies have been conducted with devices aiming at reducing aerodynamic drag. A very significative reduction in drag is described by Hucho (1987) with the use of a cab spoiler placed on top of a truck. The same reference shows several configurations using flow deflectors with a reduction in drag of up to 34%. Other devices, involving modification in rear flow characteristics did not produce significative results in drag reduction. Marks and Buckley (1978) used a combination of turning vanes distributed on the vehicle surface but produced a reduction in drag smaller than the additional drag generated by the vanes. Garry and Wong (1981) showed that it is possible to optimize the number and placement of aerodynamic devices to minimize drag. Fletcher e Stewart (1986) investigated the use of trapped vortex devices in the rear of a bus with a drag reduction of approximately 25%. Kim (2004) also studied the use of aerodynamic surfaces in the rear of a bus and obtained a 12% reduction in drag in a simulated model with a rear spoiler.

Other studies involved modifications in the external surface geometry without the addition of aerodynamic devices. Ahmed (1981) showed that the wake formed in the rear of road vehicles consisted of regions of recirculation with the formation of a pair of vortices in the longitudinal plane. He also conducted another study (Ahmed, 1983) analyzing the influence of lower rear surface inclination angle on the wake and obtained minimum drag for a 12.5° angle. Hucho (1987) describes the influence of front surface corner radius on drag. The results show that drag remains constant for radii above a certain value. The above mentioned studies show that it is possible to improve vehicle aerodynamics without violating design constraints in size or internal volume.

The objective of the present study is the computational analysis of the air flow around a 1/17.5 scale bus model. The influence of model lower rear surface slope and front geometry on drag is investigated. The commercial CFD software ANSYS^{TM} CFX^{TM} is used with the RNG κ-ε turbulence model. The software solves the Reynolds averaged Navier-

Stokes equations using a finite volume method.

2. Numerical Simulation

2.1 Governing equations

The equations governing fluid dynamics are the Reynolds averaged Navier-Stokes equations. Continuity and momentum equations are written in cartesian coordinates as follows.

Continuity:

$$\frac{\partial \rho}{\partial t} + \nabla \cdot (\rho \overline{\boldsymbol{V}}) = 0 \ . \tag{1}$$

Momentum:

$$\frac{\partial (\rho \overline{\boldsymbol{V}})}{\partial t} + \nabla \cdot (\rho \overline{\boldsymbol{V}} \otimes \overline{\boldsymbol{V}}) = \nabla \cdot (\boldsymbol{\tau} - \rho \, \overline{\boldsymbol{v} \otimes \boldsymbol{v}}) + \boldsymbol{S}_M \ . \tag{2}$$

where ρ is the air density, $\overline{\boldsymbol{V}}$ is the average component of the local velocity vector, $\boldsymbol{v}$ is the time varying component of the local velocity vector, $\rho \, \overline{\boldsymbol{v} \otimes \boldsymbol{v}}$ is the Reynolds stress tensor, $\boldsymbol{\tau}$ is the stress tensor, $\boldsymbol{S}_M$ is a momentum source and $\otimes$ is the tensor product operator, defined as

$$\boldsymbol{U} \otimes \boldsymbol{V} = \begin{bmatrix} U_x V_x & U_x V_y & U_x V_z \\ U_y V_x & U_y V_y & U_y V_z \\ U_z V_x & U_z V_y & U_z V_z \end{bmatrix} \ . \tag{3}$$

Utilization of the κ-ε turbulence model introduces two additional variables in the equations. The continuity equation does not change but the momentum equation becomes

$$\frac{\partial (\rho \overline{\boldsymbol{V}})}{\partial t} + \nabla \cdot (\rho \overline{\boldsymbol{V}} \otimes \overline{\boldsymbol{V}}) - \nabla \cdot (\mu_{eff} \, \nabla \overline{\boldsymbol{V}}) = \nabla p' + \nabla \cdot (\mu_{eff} \, \nabla \overline{\boldsymbol{V}})^T \tag{4}$$

where μ_{eff} is an effective viscosity and p' is a modified pressure given by

$$p' = p + \frac{2}{3} \rho \, \kappa \ . \tag{5}$$

The standard κ-ε turbulence model is generally used in turbulent flow analysis, neglecting the secondary strain effect. The RNG κ-ε model is used to overcome that limitation. A strain variation rate is added, to the standard κ-ε dissipation equation, to account for the anisotropic effect generated by flow separation. As a result the RNG κ-ε model is generally used in high Reynolds turbulent flow analysis, with good results and excellent convergence rate when compared with the standard κ-ε model. The kinetic energy equation for the RNG κ-ε model is the same as that for the standard κ-ε. Values for κ and ε are calculated directly from the transport differential equations. The governing equations for kinetic energy and dissipation for the RNG κ-ε model are as follows.

Turbulent kinetic energy equation:

$$\frac{\partial (\rho \, \kappa)}{\partial t} + \nabla \cdot (\rho \overline{\boldsymbol{V}} \, \kappa) = \nabla \cdot \left[\left(\mu + \frac{\mu_t}{\sigma_{\kappa_{RNG}}} \right) \nabla \kappa \right] + P_\kappa - \rho \, \varepsilon \ . \tag{6}$$

Dissipation equation:

$$\frac{\partial (\rho \, \varepsilon)}{\partial t} + \nabla \cdot (\rho \overline{\boldsymbol{V}} \, \varepsilon) = \nabla \cdot \left[\left(\mu + \frac{\mu_t}{\sigma_{\varepsilon_{RNG}}} \right) \nabla \varepsilon \right] + \frac{\varepsilon}{\kappa} (C_{\varepsilon 1_{RNG}} P_\kappa - C_{\varepsilon 2_{RNG}} \rho \, \varepsilon) \ . \tag{7}$$

where $C_{\varepsilon 1_{RNG}}$, $C_{\varepsilon 2_{RNG}}$, $\sigma_{\kappa_{RNG}}$ and $\sigma_{\varepsilon_{RNG}}$ are constants. P_κ represents turbulence production due to viscous forces, used in incompressible flow, and is calculated with

$$P_\kappa = \mu_t \nabla \overline{\boldsymbol{V}} \cdot (\overline{\boldsymbol{V}} + \overline{\boldsymbol{V}}^T) - \frac{2}{3} \nabla \cdot \overline{\boldsymbol{V}} \, (\mu_t \nabla \cdot \overline{\boldsymbol{V}} + \rho \, \kappa) \tag{8}$$

where μ_t is the turbulent viscosity. The coefficients in Eqs. (6) and (7) are defined as

$$\sigma_{\kappa_{RNG}} = \sigma_{\varepsilon_{RNG}} = 0.7179 \ , \ C_{\varepsilon 1_{RNG}} = 1.42 - f_\eta \ , \ C_{\varepsilon 2_{RNG}} = 1.68 \tag{9}$$

and

$$f_\eta = \frac{\eta \left(1 - \frac{\eta}{4.38} \right)}{1 + \beta_{RNG} \, \eta^3} \tag{10}$$

$$\eta = \sqrt{\frac{P_k}{\rho\, C_{\mu_{RNG}}\, \varepsilon}} \tag{11}$$

where

$$\beta_{RNG} = 0.012\ ,\ C_{\mu_{RNG}} = 0.085\ . \tag{12}$$

2.2 Grid generation and computational model

The bus model is placed in a computational domain to simulate the flow over the entire vehicle. The lower domain boundary represents the road surface. Model geometry is kept very simple with no representation of external elements such as rearview mirrors or air conditioning compartment. Tire and wheel representation is also simplified. An already built wind tunnel bus model, to be used in the experimental verification, also has the same simplified geometry. Bus geometry is defined using CAD software and exported in IGES (International Graphics Exchange Standard) file format. The volumetric computational grid is generated with tetrahedral elements using ANSYS^{TM} ICEM^{TM} commercial software. Air flow analysis is conducted using ANSYS^{TM} CFX^{TM} CFD commercial software which solves the previously described equations using a finite volume method. Continuity and momentum equations are solved using a high resolution method. Turbulent dissipation and kinetic energy equations are solved with an upwind method. The solution process discretization of the equations in integral form is conducted as described by Fortuna (2000). Model dimensions follow typical road bus geometry (Fig. 1) and the computational domain has the same dimensions of the wind tunnel test section, to be used in the experimental verification (Fig. 2). In the near future, experimental testing will be conducted in a wind tunnel to collect drag force and pressure distribution around the bus model, for comparison with computational results.
The air flow around the 1:17.5 scale bus model is analyzed with respect to vortex intensity in the turbulent rear wake

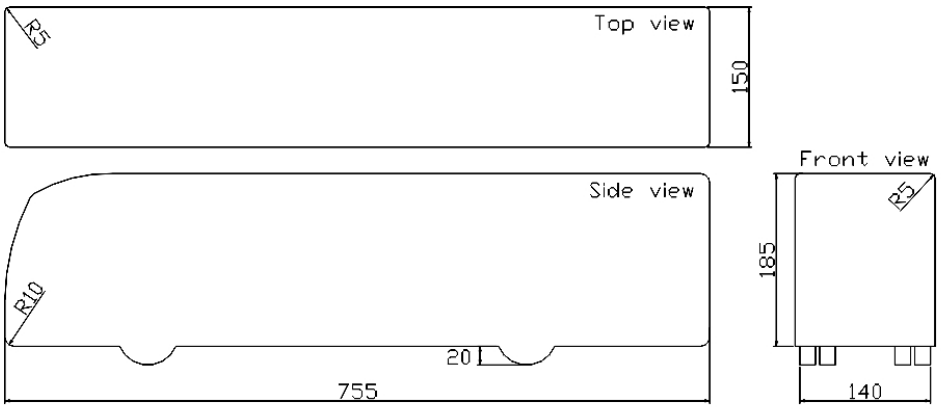

Figure 1. Bus model dimensions (mm).

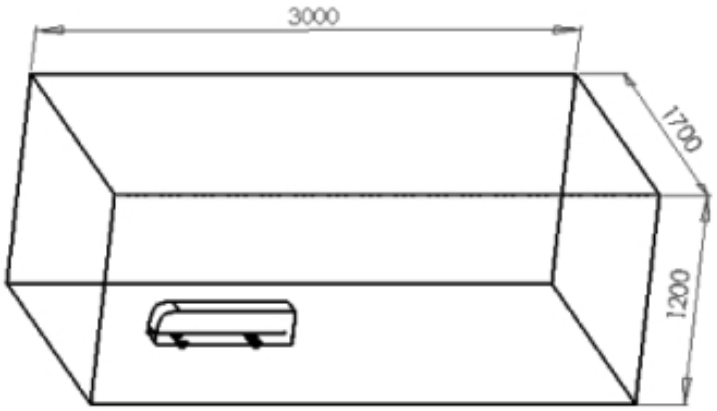

Figure 2. Dimensions of the computational domain (mm).

for different geometric configurations. Configurations A, B and C employed for the present computational analysis are

indicated in Fig. 3. Free stream air speeds are set to 23, 28 and 34 m/s, also compatible with the wind tunnel testing capabilities. Aerodynamic drag is evaluated for each configuration.

Figure 3. Bus model configurations.

3. Computational Results and Analysis

3.1 Flow characteristics in the front, rear and wake

Flow characteristics can be seen with the velocity vectors in the front and rear of the bus model in Fig. 4. A close

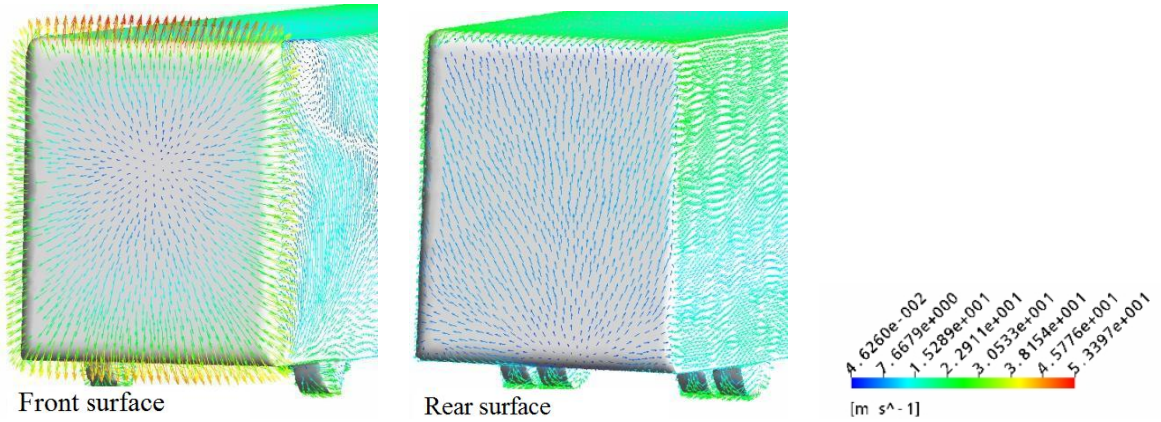

Figure 4. Velocity vectors in the front and rear for configuration A.

to stagnation area, typical of bus configurations, can be observed in the front part with corresponding increase in local pressure. That stagnation area is the main generator of aerodynamic drag. When the flow approaches the corners it rapidly accelerates with corresponding decrease in local pressure. In the rear the velocity vectors indicate that the air flows upwards in the middle/upper regions and sidewards in the lower region. Fig. 5 shows vortex behavior in the turbulent wake on vertical planes. For the Z=0 mm section, the air flow separates in the rear forming two vortices, on the top and bottom. The lower vortex is influenced by the flow passing through the bottom of the bus. Recirculation is more intense on the Z=30 mm section due to the smaller, stronger vortices. On the Z=60 mm section the air on the bottom flows mostly sidewards. Figure 6 shows the velocity vectors for horizontal planes in the bus wake. The Y=80 mm section shows two vortices with greater intensity than those on section Y=20 mm which are larger and weaker. The velocity x-component distribution is shown in Fig. 7. For the X/L=1.05 section it can be noted the absence of vortices on the bottom part. The downward flow on the top portion generates vortices but the stronger lateral flow on the bottom prevents formation of vortices on the transversal plane on the lower portion of the bus. As the distance from the rear of the bus increases, as on sections X/L=1.1 and X/L=1.15, the vortices move to the sides and to the bottom, becoming weaker.

3.2 Flow characteristics with model modifications

Computational results are obtained for configurations A, B and C. Configuration C is the baseline with an angle in the rear bottom and a rounded front portion. Configuration B excludes the rear bottom angle and configuration A excludes both the rear bottom angle and the rounded front portion. The air flow around the bus is analyzed for each configuration and the results are compared. Figure 8 shows the pressure distribution on the longitudinal symmetry plane for configuration C. The stagnation area in the front part is evident. Figure 9 shows the velocity vectors on the longitudinal symmetry plane in the wake region for configurations A, B and C. Configurations A and B show the same characteristics for the turbulent wake, both with one vortex formation on the top portion of the bus rear. For configuration C the wake

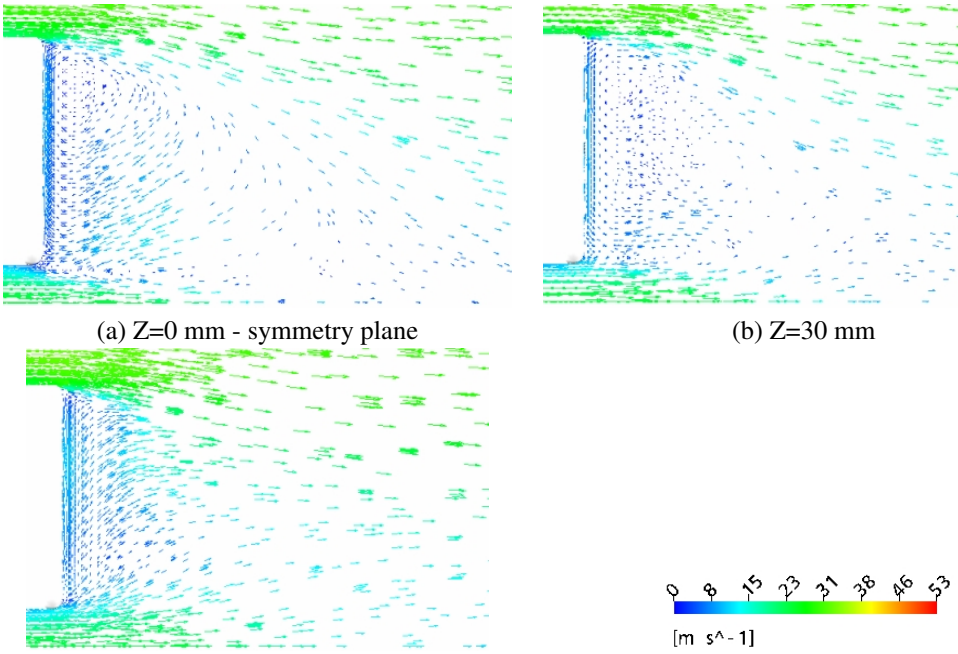

(a) Z=0 mm - symmetry plane (b) Z=30 mm

(c) Z=60 mm

Figure 5. Vertical planes in the wake for configuration A.

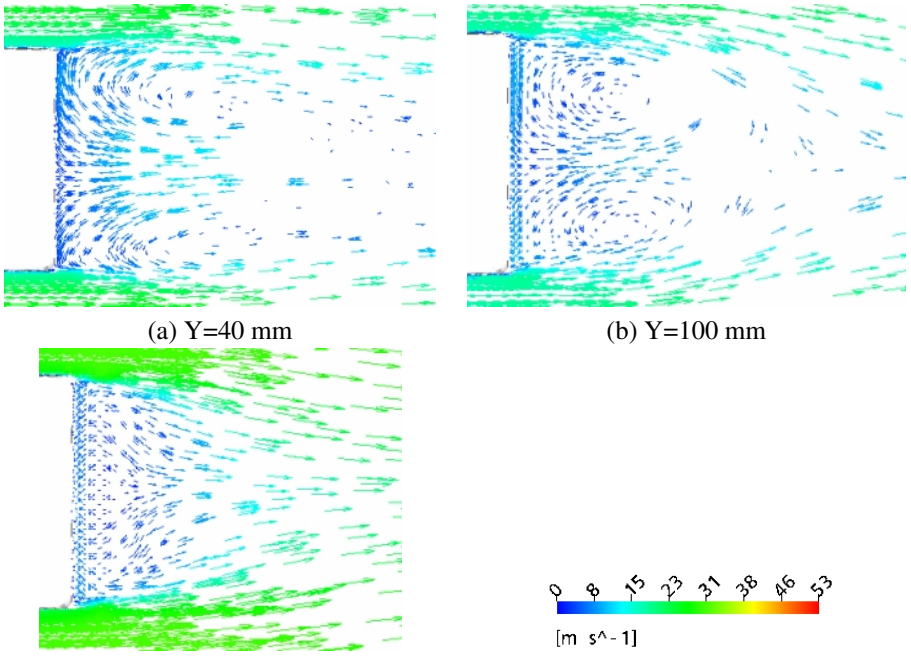

(a) Y=40 mm (b) Y=100 mm

(c) Y=180 mm

Figure 6. Horizontal planes in the wake for configuration A.

shows a decrease in wake size due to the modification in the front of the bus. That modifications resulted in a large vortex being generated in the lower portion of the bus wake.

Table 1 shows the drag coefficient for each configuration at different speeds. The results show a significative variation in drag coefficient for the different configurations with the lowest values for configuration B. The variation in drag coefficients between configurations B and C is small when compared with variations with respect to configuration A. This shows that the introduction of an angle in the rear of the bus has a much smaller contribution to drag reduction than that obtained with the rounded front portion. The results also show negligible variation in drag coefficient for the considered speed range. According to Baysal (2000) other external components such as rearview mirrors and air conditioning compartment generate a very significative increase in drag which has not been considered in the present study. The results

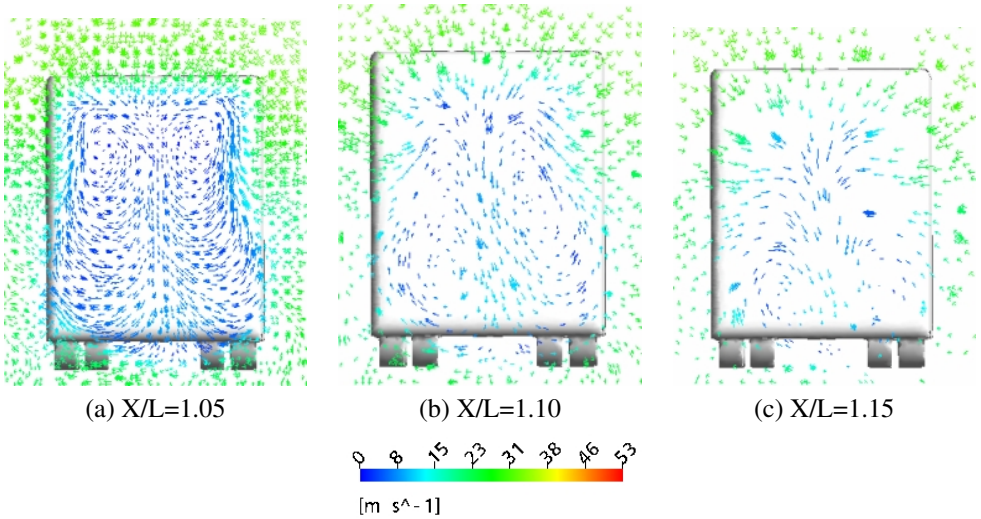

(a) X/L=1.05 (b) X/L=1.10 (c) X/L=1.15

Figure 7. Transversal planes in the wake for configuration A.

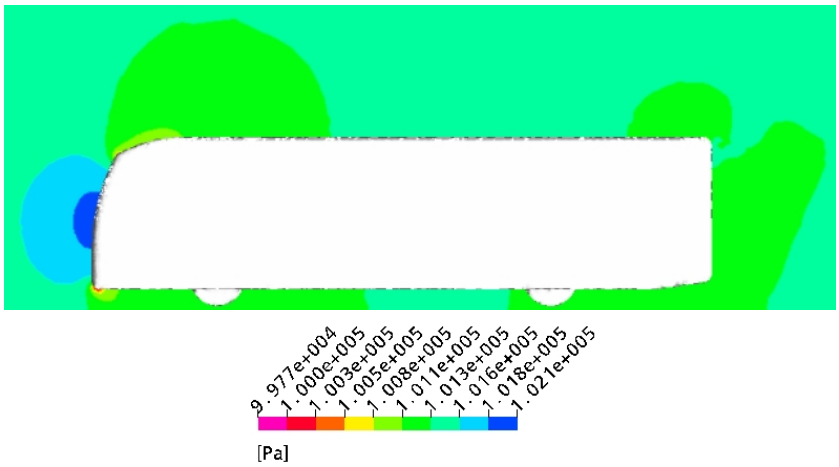

Figure 8. Pressure distribution for configuration C.

show that a large decrease in drag can be obtained with variation in bus external geometry with resulting decrease in fuel consumption.

Table 1. Drag coefficient for the three configurations.

	C_D			ΔC_D		
Velocity	Config. A	Config. B	Config. C	A-B	A-C	B-C
23 m/s	0.672	0.531	0.543	0.14 (-20%)	0.13 (-19%)	0.01 (+2%)
28 m/s	0.670	0.529	0.540	0.14 (-20%)	0.13 (-19%)	0.01 (+2%)
34 m/s	0.667	0.526	0.538	0.14 (-20%)	0.13 (-19%)	0.01 (+2%)

4. Conclusions

The three-dimensional turbulent flow around a bus model was investigated and the changes in wake and drag characteristics for different configurations were obtained computationally. The study of the flow around a bus is very complex, even with a simplified configuration, and the results should be viewed with caution. An experimental analysis will be conducted in the near future in an attempt to verify the computational results. The use of commercial CFD software is increasingly accessible both in terms of ease of use and computational cost. It offers great flexibility in testing different configurations at much lower costs when compared to experimental methods.

The modifications introduced with the different configurations showed clear tendencies for drag reduction with ex-

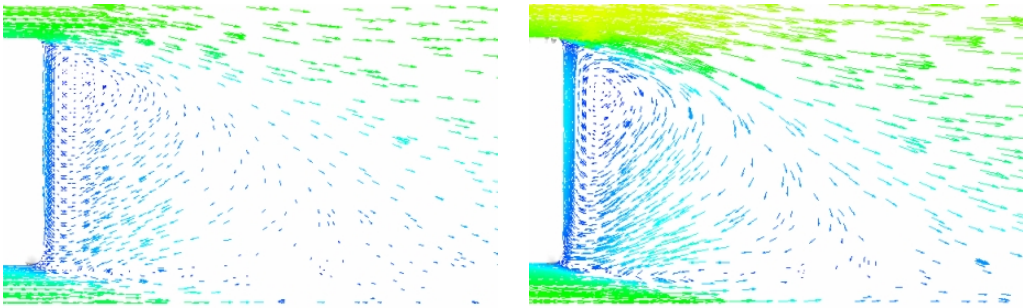

(a) Configuration A (b) Configuration B

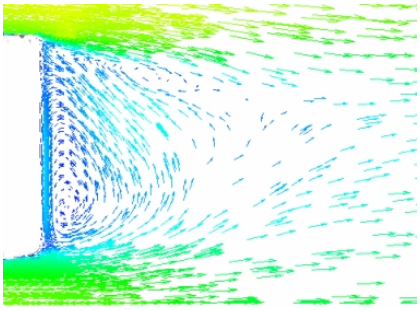

(c) Configuration C

Figure 9. Velocity vectors in the wake for the three configurations.

ternal geometry modifications. Even though those results would still have to be verified through experiments the cost associated with them could be greatly reduced.

5. Acknowledgements

The authors would like to thank CAPES for the financial support and ESSS for providing temporary software licenses for conducting the present study.

6. References

Ahmed, S.R., 1981, "Wake structure of typical automobile shapes", Journal of Fluids Engineering, Vol. 103, March 1981, pp. 162-169.

Ahmed, S.R., 1983, "Influence of base slant on the wake structure and drag of road vehicles", Journal of Fluids Engineering, Vol. 105, December 1983, pp. 429-434.

Baysal, O., Bayraktar, I., 2000, "Computational simulations for the external aerodynamics of heavy trucks", SAE Paper 2000-01-3501.

Fletcher, C.A.J., Stewart, G.D.H., 1986, " Bus drag reduction by the trapped vortex concept for a single bus and two buses in tandem", Journal of Wind Engineering and Industrial Aerodynamics, Vol 24, pp. 143-168.

Fortuna, A.O., 2000, "Técnicas Computacionais para Dinâmica dos Fluidos", EDUSP, Editora da Universidade de S.Paulo, Brazil.

Garry, K.P., 1981, "Development of container-mounted devices for reducing the aerodynamic drag of commercial vehicles", Journal of Wind Engineering and Industrial Aerodynamics, Vol 9, pp. 113-124.

Hucho, W.H, 1987, "Aerodynamics of Road Vehicles", Butterworths.

Kim, M.H., 2004, "Numerical study on the wake flow characteristics and drag reduction of large-sized bus using rear-spoiler." International Journal Vehicle Design, Vol. 34, Nř. 3.

Marks, C.H., Buckley Jr., F.T., 1978, "A wind-tunnel study of the effect of turning vanes on the aerodynamic drag of tractor-trailer trucks", Journal of Fluids Engineering, Vol. 100, December 1978, pp. 439-442.

Marks, C.H., Buckley Jr., F.T., Walston Jr., W.H. 1978, "A study of the base drag of tractor-trailer trucks", Journal of Fluids Engineering, Vol. 100, December 1978, pp. 443-448.

Wong, Y., Cox, R.N., Rajan, A., 1981, "Drag reduction of trailer-tractor configuration by aerodynamic means", Journal of Wind Engineering and Industrial Aerodynamics, Vol 9, pp. 101-111.

7. Responsibility notice

The author(s) is (are) the only responsible for the printed material included in this paper